Chapter 18

A Theoretical Model of the Holographic Formation of Controllable Waveguide Channels System in Photopolymer Liquid Crystalline Composition

Artem Semkin and Sergey Sharangovich

Additional information is available at the end of the chapter

http://dx.doi.org/10.5772/intechopen.74838

Abstract

Rapid development of the integrated optics and photonics makes it necessary to create cheap and simple technology of optical waveguide systems formation. Photolithography methods, widely used for these tasks recently, require the production of a number of precision amplitude and phase masks. This fact makes this technology expensive and the formation process long. On another side there is a cheap and one-step holographic recording method in photopolymer compositions. Parameters of the waveguide system formed by this method are determined by recording geometry and material's properties. Besides, compositions may contain liquid crystals that make it possible to create elements, controllable by external electric field. In this chapter, the theoretical model of the holographic formation of controllable waveguide channels system in photopolymer liquid crystalline composition is developed. Special attention is paid to localization of waveguides in the media caused by light field attenuation during the formation process.

Keywords: photopolymer, liquid crystal, waveguide, holography

1. Introduction

The ability to form waveguide systems for optical and terahertz radiation in photopolymerizable compositions recently is of great interest among researchers: [1–4]. Formed holographically or by photolithography methods, such waveguides are widely used in the integrated optics and photonics devices. Besides, it seems urgent to create the manageable light guides, in which the light propagation conditions can be controlled by external influences, such as an electric field.

One of the possible solutions of this problem is a holographic recording of the waveguide channels in a photopolymer composition containing liquid crystals.

The aim of this chapter is to develop the theoretical model of holographic formation of controllable waveguide channels system in photopolymer liquid crystalline composition with dye sensitizer, also known as polymer-dispersed (PDLC) or polymer-stabilized (PSLC) liquid crystals.

2. Theoretical model

We consider the incidence of two plane monochromatic waves $\mathbf{E}_0$ and $\mathbf{E}_1$ with incidence angles θ_0 and θ_1 on the PDLC (PSLC) sample for two formation geometries: transmission (**Figure 1a**) and reflection (**Figure 1b**) ones.

Thus, recording waves in the general case can be described as:

$$\begin{aligned}\mathbf{E}_0(\mathbf{r},t) &= \mathbf{e}_0 \cdot E_0(\mathbf{r}) \cdot e^{i\cdot\left(\omega t-\mathbf{k_0}\cdot\mathbf{r}-\varphi_0(\mathbf{r})\right)-\alpha(\mathbf{r},t)\cdot(\mathbf{N}_0\cdot\mathbf{r})},\\ \mathbf{E}_1(\mathbf{r},t) &= \mathbf{e}_1 \cdot E_1(\mathbf{r}) \cdot e^{i\cdot\left(\omega t-\mathbf{k}_1\cdot\mathbf{r}-\varphi_1(\mathbf{r})\right)-\alpha(\mathbf{r},t)\cdot(\mathbf{N}_1\cdot\mathbf{r}),}\end{aligned} \tag{1}$$

where $\mathbf{e}_0$, $\mathbf{e}_1$ are the unit polarizations vectors of the beams; $E_0(\mathbf{r})$, $E_1(\mathbf{r})$ are the spatial amplitude distributions; $\varphi_0(\mathbf{r})$, $\varphi_1(\mathbf{r})$ are spatial phase distributions; $\mathbf{k_0}$, $\mathbf{k}_1$ are the wave vectors; $\mathbf{N}_0$, $\mathbf{N}_1$ are wave normals; $\alpha(\mathbf{r},t)$ is the absorption coefficient; $\omega = 2\pi/\lambda$, λ is the wavelength of the recording radiation.

Investigated material is characterized by optical anisotropy properties; thus, in the material, each of recording wave (Eq. (1)) will be divided into two mutually orthogonal ones called ordinary and extraordinary. So, in the sample, Eq. (1) should be rewritten as:

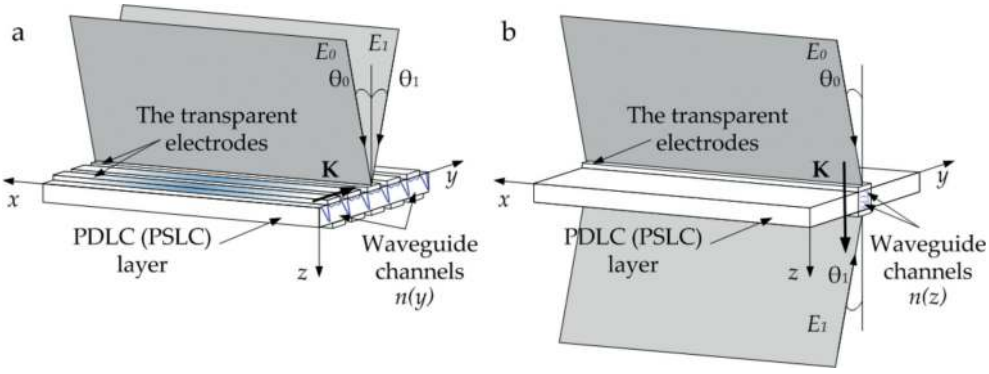

Figure 1. Waveguide channels holographic formation: (a) transmission recording geometry and (b) reflection recording geometry.

http://dx.doi.org/10.5772/intechopen.74838

$$\begin{aligned}\mathbf{E}_0(\mathbf{r},t) &= \sum_{m=o,\,e} \mathbf{e}_0^m \cdot E_0(\mathbf{r}) \cdot e^{i\cdot\left(\omega t-\mathbf{k}_0^m\cdot\mathbf{r}-\varphi_0(\mathbf{r})\right)-\alpha(\mathbf{r},t)\cdot\left(\mathbf{N}_0^m\cdot\mathbf{r}\right)},\\ \mathbf{E}_1(\mathbf{r},t) &= \sum_{m=o,\,e} \mathbf{e}_1^m \cdot E_1(\mathbf{r}) \cdot e^{i\cdot\left(\omega t-\mathbf{k}_1^m\cdot\mathbf{r}-\varphi_1(\mathbf{r})\right)-\alpha(\mathbf{r},t)\cdot\left(\mathbf{N}_1^m\cdot\mathbf{r}\right)},\end{aligned} \tag{2}$$

where $m = o$ corresponds to ordinary waves and $m = e$ corresponds to extraordinary waves, respectively.

For two recording geometries (see **Figure 1**), the spatial distributions of the forming field intensities are determined by the following expression:

$$\begin{aligned}I^T(\mathbf{r},t) &= \sum_{m=o,\,e} I^0(\mathbf{r}) \cdot e^{-\alpha(\mathbf{r},t)\cdot\left[\left(\mathbf{N}_0^m+\mathbf{N}_1^m\right)\cdot\mathbf{r}\right]} \cdot \left[1+m^m(\mathbf{r})\cos\left(\mathbf{K}^m\cdot\mathbf{r}+\varphi_0(\mathbf{r})-\varphi_1(\mathbf{r})\right)\right]\\ I^R(\mathbf{r},t) &= \sum_{m=o,\,e} I^0(\mathbf{r}) \cdot e^{\left[\frac{-\alpha(\mathbf{r},t)\cdot d}{2}\right]} \cdot \mathrm{ch}\left\{\alpha(\mathbf{r},t)\cdot\left[\left(\mathbf{N}_0^m+\mathbf{N}_1^m\right)\cdot\mathbf{r}-\frac{d}{2}\right]\right\}\cdot\left[1+m^m(\mathbf{r})\cos\left(\mathbf{K}^m\cdot\mathbf{r}+\varphi_0(\mathbf{r})-\varphi_1(\mathbf{r})\right)\right],\end{aligned} \tag{3}$$

where $I^T(\mathbf{r},t)$, $I^R(\mathbf{r},t)$ are the spatial distributions of light field intensity for transmission and reflection geometries, respectively; $I^0(\mathbf{r}) = E_0^2(\mathbf{r}) + E_1^2(\mathbf{r})$, $m^m(\mathbf{r}) = \frac{2E_0(\mathbf{r})\cdot E_1(\mathbf{r})}{E_0^2(\mathbf{r})+E_1^2(\mathbf{r})}\cdot\left(\mathbf{e}_0^m\cdot\mathbf{e}_1^m\right)$ are the local contrasts of interference patterns; $\mathbf{K}^m = \mathbf{k}_0^m - \mathbf{k}_1^m$; d is the thickness of the material.

Under the influence of light field in photopolymer liquid crystalline composition with dye sensitizer, the dye molecule absorbs a light radiation quantum with the dye radical and the primary radical initiator formation. The radical of dye is not involved in further chemical reactions and turns to colorless leuco form.

Thus, during the waveguide channel system formation, dye concentration decreases. This fact causes the light-induced decreasing of light absorption. The absorption coefficient dependence of a mount of absorbed radiation can be written as [5]:

$$-\frac{d\alpha(\mathbf{r},t)}{dt} = \beta_q\cdot\alpha_0\cdot I_{abs}(\mathbf{r},t), \tag{4}$$

where $\alpha(\mathbf{r},t) = \alpha_0\cdot K_d(\mathbf{r},t)$ is the absorption coefficient with light-induced change taken into account; $K_d(\mathbf{r},t)$ is dye concentration; α_0 is the absorption of one molecule; β_q is quantum yield of dye; and $I_{abs}(\mathbf{r},t)$ is the light intensity from Bouguer-Lambert law:

$$\begin{aligned}I_{abs}^T(\mathbf{r},t) &= \sum_{m=o,\,e} E_0^2(\mathbf{r})\cdot\left(1-e^{-\alpha(\mathbf{r},t)\cdot\left[\mathbf{N}_0^m\cdot\mathbf{r}\right]}\right)+E_1^2(\mathbf{r})\cdot\left(1-e^{-\alpha(\mathbf{r},t)\cdot\left[\mathbf{N}_1^m\cdot\mathbf{r}\right]}\right)\\ I_{abs}^R(\mathbf{r},t) &= \sum_{m=o,\,e} E_0^2(\mathbf{r})\cdot\left(1-e^{-\alpha(\mathbf{r},t)\cdot\left[\mathbf{N}_0^m\cdot\mathbf{r}\right]}\right)+E_1^2(\mathbf{r})\cdot\left(1-e^{-\alpha(\mathbf{r},t)\cdot\left[d-\mathbf{N}_1^m\cdot\mathbf{r}\right]}\right),\end{aligned} \tag{5}$$

where $I_{abs}^T(\mathbf{r},t)$, $I_{abs}^R(\mathbf{r},t)$ are defined for transmission and reflection geometries, respectively.

Then, the solution of Eq. (3) for light-induced absorption change for transmission and reflection geometries is obtained in [5] as follows:

$$\begin{aligned}\alpha_T^m(\mathbf{r},t) &= \alpha_{sub} + \alpha_0 K_{d0} \cdot e^{-\beta_q \cdot \alpha_0 \cdot \left[\left(\mathbf{N}_0^m + \mathbf{N}_1^m\right)\cdot \mathbf{r} \cdot t\right]} \\ \alpha_R^m(\mathbf{r},t) &= \alpha_{sub} + \alpha_0 K_{d0} \cdot e^{-\beta_q \cdot \alpha_0 \cdot \left[\left(\mathbf{N}_0^m \cdot \mathbf{r} + d - \mathbf{N}_1^m \cdot \mathbf{r}\right)\cdot t\right]}\end{aligned}, \tag{6}$$

where α_{sub} is the substrate absorption coefficient and K_{d0} is the initial dye concentration.

The process of waveguide channels' holographic formation is described by the kinetic equations system (KES), written for monomer concentration and refraction index [6–8]:

$$\frac{\partial M^m(\mathbf{r},t)}{\partial t} = \operatorname{div}\left[D_M^m(\mathbf{r},t)\operatorname{grad} M^m(\mathbf{r},t)\right] - K_g \cdot \left[\frac{\alpha_0 \beta K_{d0} \tau_0 I^m(\mathbf{r},t)}{K_b}\right]^{0,5} M^m(\mathbf{r},t), \tag{7}$$

$$\frac{\partial n^m(\mathbf{r},t)}{\partial t} = \delta n_p \cdot K_g \cdot \left[\frac{\alpha_0 \beta K_{d0} \tau_0 I^m(\mathbf{r},t)}{K_b}\right]^{0,5} \frac{M^m(\mathbf{r},t)}{M_n} + \delta n_{lc} \operatorname{div}\left[D_{LC}^m(\mathbf{r},t)\operatorname{grad}\frac{M^m(\mathbf{r},t)}{M_n}\right], \tag{8}$$

where M_n is the initial concentration of the monomer; K_g, K_b are parameters of the rate of growth and breakage of the polymer chain, respectively; β is the parameter of initiation reaction; τ_0 is lifetime of the excited state of the dye molecule; $D_M^m(\mathbf{r},t)$, $D_{LC}^m(\mathbf{r},t)$ are the diffusion coefficients of the monomer and liquid crystal, respectively; δn_p, δn_{lc} are weight coefficients of the contribution of photopolymerization and diffusion processes; and $I^m(\mathbf{r},t)$ is the intensity distribution (Eq. (3)).

Diffusion coefficients can be defined from the following equations:

$$\begin{aligned}D_M^m(\mathbf{r},t) &= D_{Mn}\exp\left[-s_M\left(1 - \frac{M^m(\mathbf{r},t)}{M_n}\right)\right] \\ D_{LC}^m(\mathbf{r},t) &= D_{LCn}\exp\left[-s_{LC}\left(1 - \frac{L^m(\mathbf{r},t)}{L_n}\right)\right]\end{aligned}, \tag{9}$$

where D_{Mn} and D_{LCn} are the initial diffusion coefficients, respectively; s_M, s_{LC} are rates of reduction in time; L_n, $L^m(\mathbf{r},t)$ are the initial and current concentrations of liquid crystal.

Weight coefficients δn_p and δn_{lc} from Eq. (7) are found from the Lorentz-Lorentz formula [8]:

$$\delta n_p = \frac{4\pi}{3} \cdot \frac{\left(n_{st}^2 + 2\right)}{6 n_{st}^2} \cdot \left(\alpha_M + \frac{\alpha_P}{l}\right) \cdot \frac{\rho_M}{W_M}, \tag{10}$$

$$\delta n_{lc} = \frac{4\pi}{3} \cdot \frac{\left(n_{st}^2 + 2\right)}{6 n_{st}^2} \cdot \left(\alpha_M \frac{\rho_M}{W_M} + \alpha_{LC} \frac{\rho_{LC}}{W_{LC}}\right), \tag{11}$$

where α_M, α_P, α_{LC} are the polarizability of monomer, polymer, and liquid crystal molecules, respectively; ρ_M, ρ_{LC} are the density of the monomer and liquid crystal, respectively; W_M, W_{LC} are molecular weights; l is the average length of polymeric chains; and n_{st} is the refractive index of the composition prior to the start of the recording process, determined by the Lorentz-Lorentz formula from the refractive indices of the monomer and the liquid crystal [8]:

http://dx.doi.org/10.5772/intechopen.74838

$$n_{st} = M_n \cdot \frac{n_M^2 - 1}{n_M^2 + 2} + L_n \cdot \frac{n_{LC}^2 - 1}{n_{LC}^2 + 2}, \tag{12}$$

where n_M, n_{LC} are the monomer and liquid crystal refractive indices.

Because of periodical character of the forming fields' intensities' spatial distributions, solution of KES can be found as a sum of H spatial harmonics [8]:

$$M^m(\mathbf{r},\tau) = \sum_{j=0}^{H} M_j^m(\mathbf{r},\tau)\cos(j\mathbf{K}^m\mathbf{r}), \quad n^m(\mathbf{r},\tau) = n_{st} + \sum_{j=0}^{H} n_j^m(\mathbf{r},\tau)\cos(j\mathbf{K}^m\mathbf{r}), \tag{13}$$

where $M_j^m(\mathbf{r},\tau) = \frac{1}{2\pi}\int_{-\pi}^{\pi} M_j^m(\mathbf{r},\tau)\cos(j\mathbf{K}^m\mathbf{r})\ d(\mathbf{K}^m\mathbf{r})$, $n_j^m(\mathbf{r},\tau) = \frac{1}{2\pi}\int_{-\pi}^{\pi} n_j^m(\mathbf{r},\tau)\cos(j\mathbf{K}^m\mathbf{r})\ d(\mathbf{K}^m\mathbf{r})$ are the monomer concentration and refractive index harmonics amplitudes, respectively; n_{st} is the PDLC (PSLC) refractive index at $\tau = 0$; $\tau = t/T_M^m$ is the relative time; $T_M^m = \frac{1}{D_{Mn}^m \cdot |\mathbf{K}^m|^2}$ is the components' diffusion characteristic time.

By substituting Eq. (13) to the KES (Eqs. (7 and 8)) and using the orthogonality of spatial harmonics, a system of coupled kinetic differential equations for the amplitudes of monomer concentration harmonics can be obtained for $D_M^m(\mathbf{r},t) = D_{LC}^m(\mathbf{r},t) = D_{Mn}^m$ (stable diffusion coefficients) and $K_d(\mathbf{r},t) = K_{d0}$ (stable absorption) [6]:

$$\begin{cases} \dfrac{\partial M_0^m(\mathbf{r},\tau)}{\partial\tau} = \sum\limits_{l=0}^{H} a_{0,l}^m(\mathbf{r}) M_l^m(\mathbf{r},\tau) \\ \dfrac{\partial M_1^m(\mathbf{r},\tau)}{\partial\tau} = -M_1^m(\mathbf{r},\tau) + \sum\limits_{l=0}^{H} a_{1,l}^m(\mathbf{r}) M_l^m(\mathbf{r},\tau) \\ \cdots\cdots\cdots\cdots\cdots\cdots\cdots\cdots\cdots\cdots \\ \dfrac{\partial M_H^m(\mathbf{r},\tau)}{\partial\tau} = -N^2 M_H^m(\mathbf{r},\tau) + \sum\limits_{l=0}^{H} a_{N,l}^m(\mathbf{r}) M_l^m(\mathbf{r},\tau) \end{cases}, \tag{14}$$

and also a system of differential equations for the amplitudes of refraction index harmonics:

$$\begin{cases} \dfrac{\partial n_0^m(\mathbf{r},\tau)}{\partial\tau} M_n = -\delta n_p \sum\limits_{l=0}^{H} a_{0,l}^m(\mathbf{r}) M_l^m(\mathbf{r},\tau) \\ \dfrac{\partial n_1^m(\mathbf{r},\tau)}{\partial\tau} M_n = -\delta n_p \sum\limits_{l=0}^{H} a_{1,l}^m(\mathbf{r}) M_l^m(\mathbf{r},\tau) + \delta n_{lc} M_1^m(\mathbf{r},\tau) \\ \cdots\cdots\cdots\cdots\cdots\cdots\cdots\cdots\cdots\cdots\cdots\cdots\cdots\cdots \\ \dfrac{\partial n_H^m(\mathbf{r},\tau)}{\partial\tau} M_n = -\delta n_p \sum\limits_{l=0}^{H} a_{H,l}^m(\mathbf{r}) M_l^m(\mathbf{r},\tau) + \delta n_{lc} H^2 M_H^m(\mathbf{r},\tau) \end{cases}. \tag{15}$$

In equation systems Eqs. (14) and (15), a coefficient matrix is introduced [6]:

$$a_{j,l}^{m}(\mathbf{r}) = -\begin{Bmatrix} e_1^m & e_2^m & e_3^m & 0 & 0 & 0 & . & 0 & 0 & 0 & 0 \\ 2e_2^m & e_{11}^m & e_2^m & e_3^m & 0 & 0. & . & 0 & 0 & 0 & 0 \\ 2e_3^m & e_2^m & e_1^m & e_2^m & e_3^m & 0 & . & 0 & 0 & 0 & 0 \\ 0 & e_3^m & e_2^m & e_1^m & e_2^m & e_3^m & . & 0 & 0 & 0 & 0 \\ 0 & 0 & e_3^m & e_2^m & e_1^m & e_2^m & . & 0 & 0 & 0 & 0 \\ 0 & 0 & 0 & e_3^m & e_2^m & e_1^m & . & 0 & 0 & 0 & 0 \\ . & . & . & . & . & . & . & . & . & . & . \\ 0 & 0 & 0 & 0 & 0 & 0 & . & e_1^m & e_2^m & e_3^m & 0 \\ 0 & 0 & 0 & 0 & 0 & 0 & . & e_2^m & e_1^m & e_2^m & e_3^m \\ 0 & 0 & 0 & 0 & 0 & 0 & . & e_3^m & e_2^m & e_1^m & e_2^m \\ 0 & 0 & 0 & 0 & 0 & 0 & . & 0 & e_3^m & e_2^m & e_1^m \end{Bmatrix}, \tag{16}$$

where $e_1^m = \frac{\sqrt{2}}{b_s^m}\left(1 + L_s^m\right)$; $e_{11}^m = \frac{\sqrt{2}}{b_s^m}\left(1 + 3L_s^m/2\right)$; $e_2^m = \frac{\sqrt{2}m_s^m}{4b_s^m}$; $e_3^m = \frac{\sqrt{2}}{b_s^m}L_s^m/2$; $m_s^m = m^m(\mathbf{r})$; $L_s^m = L^m(\mathbf{r}) = -[m^m(\mathbf{r})]^2/16$; $b_s^m = b^m(\mathbf{r}) = \frac{T_p^m(\mathbf{r})}{T_M^m(\mathbf{r})}$ are the parameters that characterize the ratio of polymerization and diffusion rates; and $T_p^m(\mathbf{r})$ is the characteristic polymerization time:

$$T_p^m(\mathbf{r}) = \frac{1}{K_g} \cdot \left[\frac{2K_b}{\alpha_0 \beta K_{d0} \tau_0 I^m(\mathbf{r})}\right]^{0,5}, \tag{17}$$

$T_M^m(\mathbf{r})$ is the characteristic diffusion time:

$$T_M^m(\mathbf{r}) = \frac{1}{D_{Mn}^m \cdot \left[\mathbf{K}^m \cdot \mathbf{r} + \varphi_0(\mathbf{r}) - \varphi_1(\mathbf{r})\right]^2}. \tag{18}$$

Coefficients $a_{j,l}^m(\mathbf{r})$ describe the contributions of photopolymerization and diffusion recording mechanisms. However, for analysis of equation systems Eqs. (14) and (15), it is convenient to introduce the coupling coefficients $c_{j,l}^m(\mathbf{r}) = a_{j,l}^m(\mathbf{r}) - j^2\delta_{j,l}$ ($\delta_{j,l}$ is the Kronecker symbol), which characterizes the coupling between j and l harmonics. The difference between coefficients $c_{j,l}^m(\mathbf{r})$ and $a_{j,l}^m(\mathbf{r})$ characterizes the contribution of monomer diffusion to the recording process and it is proportional to the second degree of the harmonic's number. The increase of this contribution according to the harmonic's number is due to grating period decrease and, respectively, the diffusion characteristic time decrease for this harmonic.

For solution of the coupled differential equations system (14), the initial conditions should be introduced:

$$M_0^m(\mathbf{r}, \tau = 0) = M_n, M_1^m(\mathbf{r}, \tau = 0) = 0, \ldots, M_H^m(\mathbf{r}, \tau = 0) = 0. \tag{19}$$

The solution can be found using the operator method [6]. The general solution for the spatial amplitude profiles of monomer concentration harmonics will be:

$$M_j^m(\mathbf{r},\tau) = M_n \sum_{l=0}^{H} A_{j,l}^m(\mathbf{r}) \exp\left[\lambda_l^m(\mathbf{r})\cdot\tau\right], \tag{20}$$

where functional dependencies of coefficients $\lambda_l^m(\mathbf{r})$ are defined as the roots of the characteristic equation $\left|c_{j,l}^m(\mathbf{r}) - \lambda_l^m(\mathbf{r})\right| = 0$. Analysis shows that $\lambda_l^m(\mathbf{r})$ is real, different, and negative. Coefficients $A_{j,l}^m(\mathbf{r})$ are defined as solutions of a system of linear algebraic equations:

$$\begin{Bmatrix} 1 & 1 & 1 & . & 1 \\ \lambda_0^m & \lambda_1^m & \lambda_2^m & . & \lambda_H^m \\ \lambda_0^{m^2} & \lambda_1^{m^2} & \lambda_2^{m^2} & . & \lambda_H^{m^2} \\ \lambda_0^{m^3} & \lambda_1^{m^3} & \lambda_2^{m^3} & . & \lambda_H^{m^3} \\ \lambda_0^{m^4} & \lambda_1^{m^4} & \lambda_2^{m^4} & . & \lambda_H^{m^4} \\ . & . & . & . & . \\ \lambda_0^{m^H} & \lambda_1^{m^H} & \lambda_2^{m^H} & . & \lambda_H^{m^H} \end{Bmatrix} \times \begin{Bmatrix} A_{j,0}^m \\ A_{j,1}^m \\ A_{j,2}^m \\ A_{j,3}^m \\ A_{j,4}^m \\ \cdots \\ A_{j,H}^m \end{Bmatrix} = M_n \begin{Bmatrix} \delta_{j,0} \\ c_{j,0}^m \\ \sum\limits_{i_0=0}^{H} c_{j,i_0}^m c_{i_0,0}^m \\ \sum\limits_{i_1=0}^{H} c_{j,i_1}^m \sum\limits_{i_0=0}^{H} c_{i_1,i_0}^m c_{i_0,0}^m \\ \cdots\cdots\cdots\cdots\cdots\cdots\cdots\cdots\cdots\cdots \\ \sum\limits_{i_{(N-2)}=0}^{H} c_{j,i_{N-1}}^m \ldots \sum\limits_{i_2=0}^{H} c_{i_3,i_2}^m \sum\limits_{i_1=0}^{H} c_{i_2,i_1}^m \sum\limits_{i_0=0}^{H} c_{i_1,i_0}^m c_{i_0,0}^m \end{Bmatrix}, \tag{21}$$

where $\lambda_l^m = \lambda_l^m(\mathbf{r})$, $A_{j,l}^m = A_{j,l}^m(\mathbf{r})$, $c_{j,l}^m = c_{j,l}^m(\mathbf{r})$.

Then, by substituting (20) to (15) and by integrating the resulting differential equations with initial conditions, we get.

$$n_0^m(\mathbf{r},\tau=0) = 0, n_1^m(\mathbf{r},\tau=0) = 0, \ldots n_H^m(\mathbf{r},\tau=0) = 0 \tag{22}$$

The general solution for the amplitude of j-harmonic of the refractive index can be found:

$$n_j^m(\mathbf{r},\tau) = n_{pj}^m(\mathbf{r},\tau) + n_{lcj}^m(\mathbf{r},\tau), \tag{23}$$

where $n_{pj}^m(\mathbf{r},\tau) = \delta n_p \sum\limits_{l=0}^{H} a_{j,l}^m(\mathbf{r}) \sum\limits_{q=0}^{H} A_{l,q}^m(\mathbf{r}) \frac{1-\exp\left[\lambda_q^m(\mathbf{r})\cdot\tau\right]}{\lambda_q^m(\mathbf{r})}$, $n_{lcj}^m(\mathbf{r},\tau) = -\delta n_{lc}\cdot j^2 \sum\limits_{q=0}^{H} A_{j,q}^m(\mathbf{r}) \frac{1-\exp\left[\lambda_q^m(\mathbf{r})\cdot\tau\right]}{\lambda_q^m(\mathbf{r})}$, $j = 0,\ldots,H$.

Thus, Eqs. (13), (20), and (23) are the general solutions of nonlinear photopolymerization diffusion holographic recording of waveguide channels system in PDLCs (PSLCs) in the case of stable diffusion coefficients and stable absorption. They define kinetics of spatial profiles of monomer concentration—$M^m(\mathbf{r},\tau)$ and refractive index $n^m(\mathbf{r},\tau)$.

In case of high nonlinearity, it is possible to form the specific spatial profile of refractive index. The nonlinearity of recording is achieved by changing the ratio of the photopolymerization and diffusion mechanism contributions to the process of structure's formation.

3. Numerical simulations

To investigate the formation processes, numerical simulations of first four refractive index harmonics kinetics for transmission and reflection geometries were made with the following parameters: $\lambda = 633$ nm and $\theta_0 = -\theta_1 = 30^\circ$ for transmission geometry (**Figure 1a**) and $\theta_0 = -\theta_1 = 60^\circ$ for reflection geometry (**Figure 1b**); $E_0(\mathbf{r}) = E_1(\mathbf{r}) = 1$; $\varphi_0(\mathbf{r}), = \varphi_1(\mathbf{r}) = 0$; $\mathbf{e}_0$, $\mathbf{e}_1$ are oriented with respect to extraordinary waves in material; $d = 10$ μm; $\delta n_p/\delta n_i = 0.5$; and for two values of parameter $b = b^e = 0.2$ and $b = b^e = 5$ in the absence of absorption. Values $b = 0.2$ and 5 are chosen as an example to investigate two common cases: $b << 1$ and $b >> 1$. Simulations were made by Eq. (23); results are shown in **Figure 2**.

As can be seen from **Figure 2**, in the case of predomination of polymerization ($b^e = 0.2$, **Figure 2a**), the structure forms quickly, but amplitudes of higher harmonics are high, so the spatial profile of refractive index changes has an inharmonic character. In another case of diffusion predominance ($b^e = 5$, **Figure 2b**), spatial profile is quasi-sinusoidal, but it is slower. These effects can be explained by the following. When polymerization is rapid, in the area of the maximum of intensity distribution (Eq. (3)), molecules of liquid crystal do not have time to diffuse, so the concentrations' gradient is not high enough; monomer molecules do not diffuse from minimums of intensity distribution. Thus, profile of refractive index distribution becomes inharmonic. So, it can be concluded that ratio of polymerization and diffusion rates $b^m(\mathbf{r}, \tau)$ defines the distribution $n^m(\mathbf{r}, \tau)$.

Corresponding distributions $n^e(\mathbf{r}, \tau = 50)$ for two examined cases in the absence of absorption are shown in **Figure 3**.

In **Figure 3**, a new spatial coordinate is introduced: $\xi = y$ for transmission geometry (see **Figure 1a**) and $\xi = z$ for reflection geometry (see **Figure 1b**).

According to Eqs. (17) and (18), parameter $b^m(\mathbf{r}, \tau)$ depends on formation field's amplitude and phase distributions as well as material properties. So, by controlling these parameters one can create any distribution of refractive index $n^m(\mathbf{r}, \tau)$. As is shown in **Figure 3**, distributions can be quasi-rectangular (**Figure 3a**) and quasi-sinusoidal (**Figure 3b**), so they can be mentioned as waveguides systems.

It should be also noted that the amplitude of refractive index change when $b = 0.2$ (**Figure 3a**), due to high amplitudes of higher harmonics (see **Figure 2a**), is lower than in the case of $b = 5$.

To investigate the impact of absorption on the spatial profile of structure along the thickness of the sample, numerical simulations were made with the following parameters: $\lambda = 633$ nm; $\theta_0 = -\theta_1 = 30^\circ$ for transmission geometry (**Figure 1a**) and $\theta_0 = -\theta_1 = 60^\circ$ for reflection geometry (**Figure 1b**); $E_0(\mathbf{r}) = E_1(\mathbf{r}) = 1$; $\varphi_0(\mathbf{r}), = \varphi_1(\mathbf{r}) = 0$; $\mathbf{e}_0$, $\mathbf{e}_1$ are oriented with respect to extraordinary waves in material; $d = 10$ μm; $\delta n_p/\delta n_i = 0.5$; $b = b^e = 5$; $\alpha d = 2$ *Np*. Simulations were made by Eq. (23) for the amplitude of the first harmonic of refractive index and for two formation geometries. Results are shown in **Figure 4**.

http://dx.doi.org/10.5772/intechopen.74838

As shown in **Figure 4**, absorption of the formation field causes dependence of the first harmonic on *z*-coordinate (see **Figure 1**) during the recording process. Thus, the spatial profile of refractive index changes its character in time and space.

In **Figure 4**, some characteristic cases of localization of maximum of refractive index change in the thickness can be seen. In particular, in the case of transmission geometry (**Figure 4a**) at $\tau = 2.5$, maximum is localized between 1.5 and 3.5 μm of the material thickness. For reflection geometry (**Figure 4b**), one maximum is localized near 5 μm at $\tau = 1.25$, and there are two

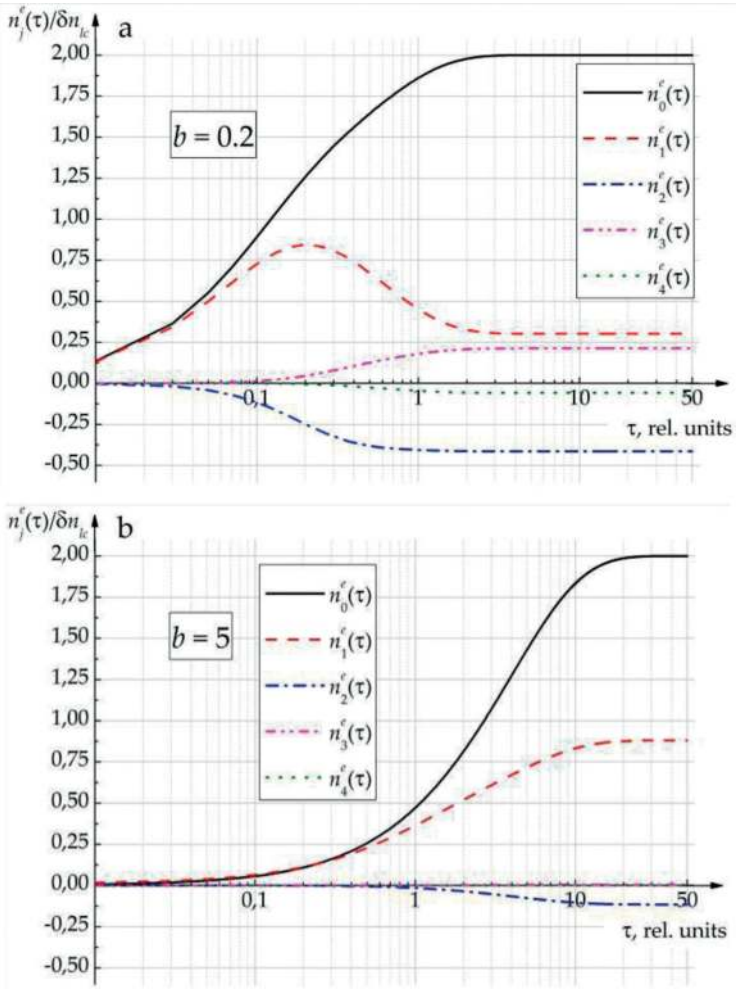

Figure 2. Refractive index harmonics kinetics for $b = 0.2$ (a) and $b = 5$ (b).

other maximums at $\tau > 2.5$. These effects take place because of dependence $b^m(\mathbf{r})$. Absorption causes the dependence on z-coordinate and spatial distributions of amplitude, and the phase of recording field (Eqs. (1) and (2)) causes the dependence on x and y coordinates. In more general cases, there is also a temporal dependence $b^m(\mathbf{r}, \tau)$ caused by photo-induced effects (Eq. (6)).

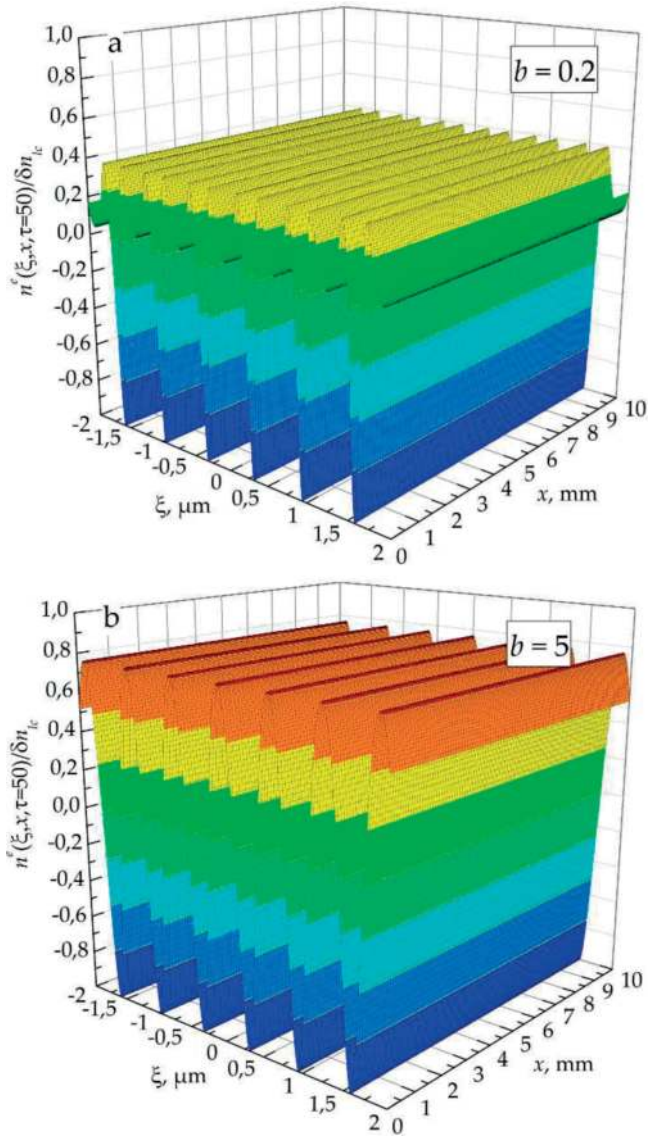

Figure 3. Refractive index distributions for $b = 0.2$ (a) and $b = 5$ (b).

http://dx.doi.org/10.5772/intechopen.74838

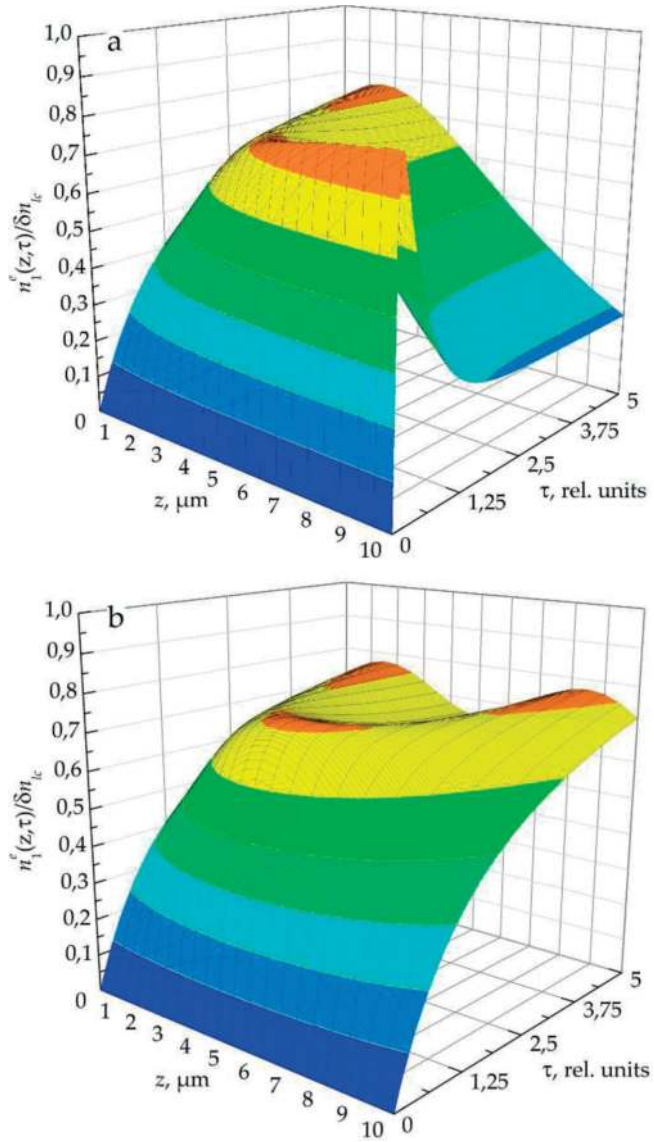

Figure 4. Impact of light absorption: transmission geometry (a) and reflection geometry (b).

To illustrate the localization of waveguide channels into the material, in **Figure 5**, there are some more two-dimensional spatial distributions of refractive index, obtained by Eq. (23) for transmission and reflection geometries—$b = b^e = 5$ and for different values of τ.

It follows from the abovementioned that by controlling the spatial distribution of light field and taking the absorption effects into account, the waveguide systems localized into the

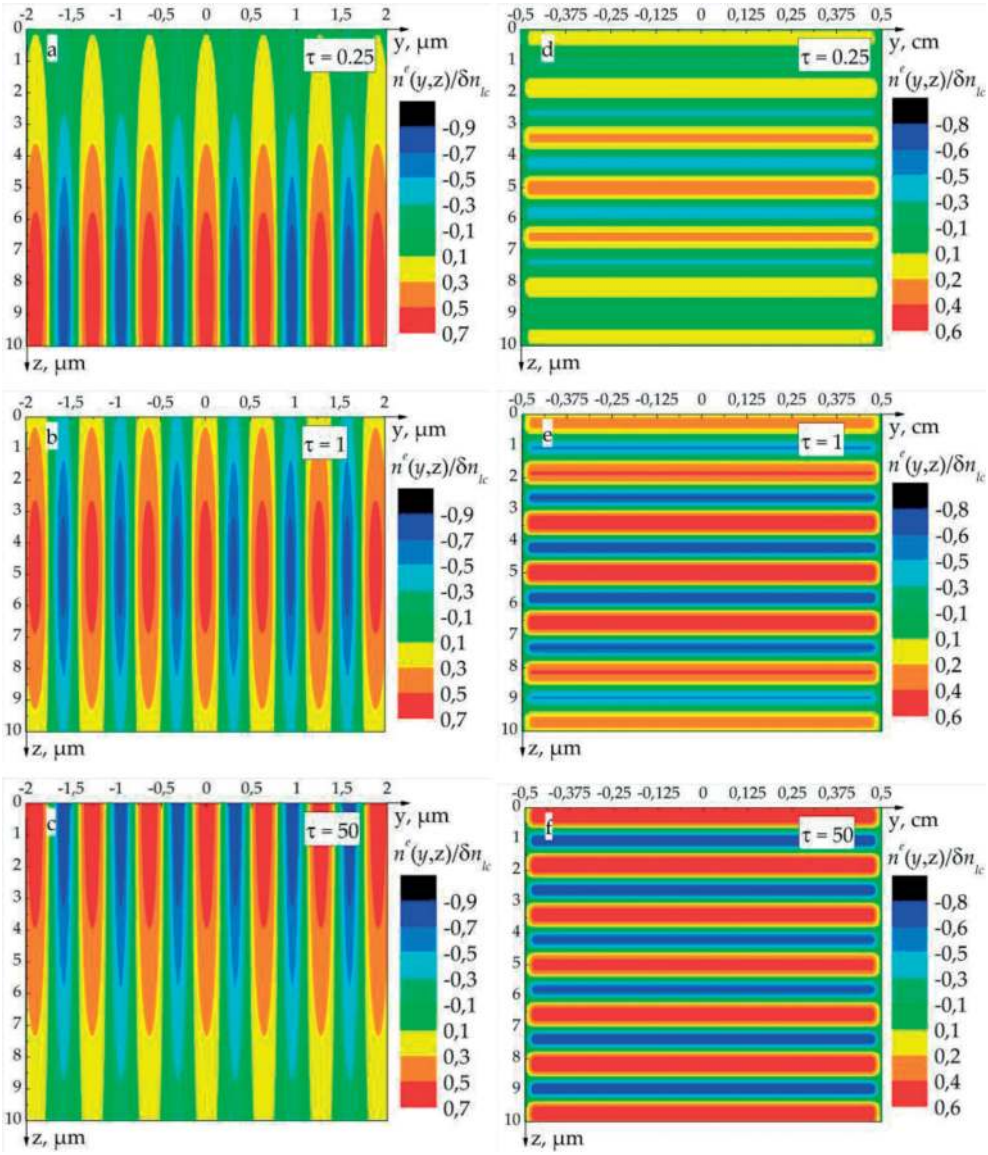

Figure 5. Two-dimensional refractive index distributions: transmission geometry (a–c) and reflection geometry (d–f).

material can be holographically formed. Localization is important because of the necessity to create a predetermined refractive index profile independent from properties of possible substrates (electrodes, glass, polymer layers, etc.). In particular, to create the waveguide system localized near the bottom substrate, formation geometry should be transmissive and formation

http://dx.doi.org/10.5772/intechopen.74838

should be stopped before $\tau = 0.5$, for localization into the center of the sample—$0.5 < \tau < 2.5$—for transmission and reflection geometries, and for $\tau > 2.5$, waveguides will be localized near the top substrate for transmission geometry and not localized for reflection geometry. The given values of τ are valid for the formation parameters given earlier.

In our recent works [9–18], we have seen that the impact of the external electric field on the holographic structure formed in PDLC (PSLC) leads to the refractive index change due to electro-optical orientation mechanisms, that is typical to liquid crystals, and the recorded structure can be "erased". So, it can be supposed that the impact of external electric field on individual waveguides will lead to its "erasing", and it is possible to "switch off" some waveguides or change the system's period, and so on.

4. Conclusion

Thus, in this chapter, the theoretical model of holographic formation of controllable waveguide channels system in photopolymer liquid crystalline composition is developed. The most general cases are described by the developed model, and numerical simulations were made for plane recording waves and stable absorption cases. Special attention is paid to localization of waveguides in the media caused by light field attenuation during the formation process.

It is shown that parameters of the waveguide system formed by holography's methods are determined by recording geometry and material's properties. Also, by control of these parameters, waveguides can be localized into the sample that makes them independent from substrates. Also, introduced compositions contain liquid crystals that make it possible to create elements, controllable by external electric field.

Obtained results can be used for new photonics devices based on photopolymer liquid crystalline composition development.

Acknowledgements

The work is performed as a project that is part of Government Task of Russian Ministry of Education (project No. 3.1110.2017/4.6).

Author details

Artem Semkin and Sergey Sharangovich*

*Address all correspondence to: shr@tusur.ru

Tomsk State University of Control Systems and Radioelectronics, Tomsk, Russia

References

[1] Keil N, Zawadski C, Zhang Z, Wang J, Mettbach N, Grote N, Schell M. Polymer PLC as an Optical Integration Bench. Optical Fiber Communication Conference and Exposition (OFC/NFOEC) and the National Fiber Optic Engineers Conference. 2011;**2011**:1-3

[2] Li H, Qi Y, Mallah R, Sheridan J. Modeling the nonlinear photoabsorptive behavior during self-written waveguide formation in a photopolymer. JOSA B. 2015;**32**:912-922. DOI: 10.1364/JOSAB.32.000912

[3] Zhang Z, Felipe D, Katopodis V, Groumas P, Kouloumentas Ch, et al. Hybrid photonic integration on a polymer platform. Photonics. 2015;**2**:1005-1026. DOI: 10.3390/photonics2031005

[4] Zhang Z, Mettbach N, Zawadski C, Wang J, Schmidt D, Brinker W, Grote N, Schell M, Keil N. Polymer-based photonic toolbox: Passive components, hybrid integration and polarisation control. IET Optoelectronics. 2010;**5**:226-232. DOI: 10.1049/iet-opt.2010.0054

[5] Dovolnov E, Ustyuzhanin S, Sharangovich S. Formation of holographic transmission and reflecting gratings in photopolymers under light-induced absorption. Russian Physics Journal. 2006;**49**:1129-1138. DOI: 10.1007/s11182-006-0233-3

[6] Dovolnov E, Sharangovich S. Nonlinear model of record and readout of holographic transmission diffraction gratings in absorbent photopolymers. Part I. Theoretical analysis. Russian Physics Journal. 2005;**48**:501-510. DOI: 10.1007/s11182-005-0159-1

[7] Dovolnov E, Sharangovich S. Nonlinear model of record and readout of holographic transmission diffraction gratings in absorbent photopolymers. Part II. Numerical modelling and experiment. Russian Physics Journal. 2005;**48**:766-774. DOI: 10.1007/s11182-005-0199-6

[8] Dovolnov E, Sharangovich S. Analysis of dynamics of holographic grating formation withinharmonic spatial distribution in photopolymer + liquid crystalcompounds. Proceedings of SPIE. 2005;**6023**:602301. DOI: 10.1117/12.646947

[9] Ustyuzhanin S, Nozdrevatykh B, Sharangovich S. Anisotropic light beam diffraction on electrical controlled holographic gratings in photopolymer-dispersed liquid crystals. International Conference on Advanced Optoelectronics and Lasers (CAOL), IEEE. 2008: 407-409. DOI: 10.1109/CAOL.2008.4671969

[10] Ustyuzhanin S, Nozdrevatykh B, Sharangovich S. Transfer functions of nonuniform transmission photonic structures in polymer-dispersed liquid-crystal materials. Physics of Wave Phenomena. 2010;**18**:289-293. DOI: 10.3103/S1541308X10040102

[11] Ustyuzhanin S, Sharangovich S. Analytical model of light beam diffraction by one-dimensional electrically controlled non-uniform transmission photon PDLC structures. Russian Physics Journal. 2011;**54**:172-179. DOI: 10.1007/s11182-011-9595-2

[12] Semkin A, Sharangovich S. Diffraction characteristics of the PDLC photonic structures under the influence of alternating electric fields. Bulletin of Russian Academy of Sciences: Physics. 2013;**77**:1416-1419. DOI: 10.3103/S1062873813120125

[13] Semkin A, Sharangovich S. The analytical model of light beams diffraction on the holographic photonic PDLC structure under the influence of an alternating electric field. Pacific Science Review A. 2013;**15**:118-124

[14] Semkin A, Sharangovich S. The PDLC photonic structures diffraction characteristics managing by the spatially non-uniform electric field. International Conference on Advanced Optoelectronics and Lasers (CAOL), IEEE. 2013:48-49. DOI: 10.1109/CAOL.2013.6657522

[15] Semkin A, Sharangovich S. Analytical model of light beam diffraction on holographic polarization spatially inhomogeneous photonic PDLC structures. Physics Procedia. 2015; **73**:41-48. DOI: 10.1016/j.phpro.2015.09.119

[16] Semkin A, Sharangovich S. Light beam diffraction on inhomogeneous holographic photonic PDLC structures under the influence of spatially non-uniform electric field. Journal of Physics: Conference Series. 2016;**735**:012030. DOI: 10.1088/1742-6596/735/1/012030

[17] Semkin A, Sharangovich S. Highly effective light beam diffraction on holographic PDLC photonic structure, controllable by the spatially inhomogeneous electric field. Physics Procedia. 2017;**86**:160-165. DOI: 10.1016/j.phpro.2017.01.011

[18] Semkin A, Sharangovich S. Theoretical model of controllable waveguide channels system holographic formation in photopolymer-liquid crystalline composition. Physics Procedia. 2017;**86**:181-186. DOI: 10.1016/j.phpro.2017.01.020